Journal of Sound and Vibration (1998) **212**(5), 889–903

A FRACTIONAL DERIVATIVE RAILPAD MODEL INCLUDED IN A RAILWAY TRACK MODEL

Å. FENANDER

Division of Solid Mechanics, Chalmers University of Technology, S-412 96 Göteborg, Sweden

(*Received* 28 *April* 1997, *and in final form* 5 *January* 1998)

When studying the dynamic behaviour of a railway track, the accurate modelling of the behaviour of railpads is important. Here a fractional derivative railpad model is included in a railway track model. The response of the track model to a force traversing the track at a constant speed is calculated by use of a time integration method. Both a constant traversing force and a force modelled as a stochastic process are studied. For comparison an ordinary railpad model with a discrete elastic spring and a discrete viscous damper in parallel is also used in the track model. The calculated displacements when using the two different models are similar. A non-linear railpad model is also implemented, and is found to result in a slightly different response.

1. INTRODUCTION

A modern railway track is built up of rails fastened onto concrete sleepers which rest on the ballast. Railpads are inserted between the rails and the sleepers. The railpads protect the sleepers from wear and provide electrical insulation. They also affect the dynamic behaviour of the whole track since the stiffness and damping of the track are influenced by the properties of the railpads.

An overview of railway track models has been given by Knothe and Grassie [1]. Both frequency domain models and time domain models are in use. A benchmark test to compare some of the models has been performed, see reference [2]. Time domain models are often studied by use of modal analysis methods, as has been done by, e.g. Clark *et al*. [3], Cai and Raymond [4] and Nielsen and Abrahamsson [5].

Grassie *et al*. [6] compared calculated results from different track models with measurements. They showed that it is important to include the railpad to obtain an accurate track model. Grassie and Cox [7] pointed out the importance of the railpads when calculating the strain in the sleepers. Dalenbring [8] found that very soft pads will isolate the sleepers from the rail. Full-scale experiments with a moving train were reported by Fermér and Nielsen [9]. The influence of soft and stiff railpads on the wheel/rail contact force, on the sleeper end acceleration, and on the railhead acceleration was measured.

Hitherto the railpads have often been modelled as a discrete spring and a discrete viscous damper in parallel. Fenander [10] suggested a fractional derivative railpad model to better take into account the frequency-dependent properties of the railpads. The fractional derivative railpad model will here be included in a track model. The response to a load traversing the track model at a constant speed will be calculated by use of a time integration algorithm. One aim of the study is to compare results for the fractional derivative railpad model to results when the ordinary spring and damper model is used.

0022–460X/98/200889 + 15 $25.00/0/sv971483

A non-linear railpad model will also be studied. Another aim is to indicate a way to incorporate a fractional derivative model into a model of a complete structure.

2. FRACTIONAL DERIVATIVE MODEL

There are several different damping or viscoelasticity models in use. One common model is the viscous model where the loss factor is proportional to frequency. At high frequencies the loss factor then becomes very large, which is not realistic for many materials. The hysteretic model, on the other hand, has a frequency-independent loss factor. This model, however, leads to non-causal responses to transient loads [11]. A model which has been found to work well over a large frequency range for many materials is the fractional derivative model of viscoelasticity [12]. This linear model has a moderate loss factor at high frequencies and results in causal responses to transient loads.

In its simplest uniaxial form the fractional derivative model includes only four parameters, which are often enough to accurately describe a real material. The relationship between a tensile force $f(t)$ in the material and the corresponding elongation $x(t)$ is then written

$$f(t) + l\mathrm{D}^{\alpha} f(t) = k_0 x(t) + k_{\alpha}\mathrm{D}^{\alpha} x(t), \qquad 0 < \alpha < 1. \tag{1}$$

Here D^{α} denotes the fractional derivative of order α, with respect to time t. The order α of the two derivatives together with the factors l, k_0 and k_{α} are the four material parameters which are to be determined to fit experimental data.

The fractional derivative of order α, for α between zero and one, of a function $x(t)$ is often defined as [13],

$$\mathrm{D}^{\alpha} x(t) = \frac{1}{\Gamma(1-\alpha)} \frac{\mathrm{d}}{\mathrm{d}t} \int_0^t \frac{x(\tau)}{(t-\tau)^{\alpha}} \,\mathrm{d}\tau, \qquad 0 < \alpha < 1, \tag{2}$$

where Γ is the gamma function. One property of the fractional derivative is that the Fourier transform of the fractional derivative of a function which is zero for negative times t equals $(\mathrm{i}\omega)^{\alpha}$ times the Fourier transform of the function itself. Denoting the Fourier transform of x by $\hat{x}$, the Fourier transform of the fractional derivative of x is written as

$$\widehat{\mathrm{D}^{\alpha} x}(\omega) = (\mathrm{i}\omega)^{\alpha} \hat{x}(\omega). \tag{3}$$

The principal root of $(\mathrm{i}\omega)^{\alpha}$ should be used, see reference [14]. The Fourier transform $\hat{x}(\omega)$ of a function $x(t)$ is here defined as

$$\hat{x} = \int_{-\infty}^{\infty} x(t)\, \mathrm{e}^{-\mathrm{i}\omega t} \,\mathrm{d}t. \tag{4}$$

For a viscoelastic spring which is modelled by use of fractional derivatives, the complex-valued stiffness $k^*(\omega)$ in the frequency domain may be obtained by taking the Fourier transform of equation (1), yielding

$$k^*(\omega) = \frac{\hat{f}(\omega)}{\hat{x}(\omega)} = \frac{k_0 + k_{\alpha}(\mathrm{i}\omega)^{\alpha}}{1 + l(\mathrm{i}\omega)^{\alpha}}. \tag{5}$$

The loss factor of the spring is then obtained as the ratio of the imaginary part of its stiffness and the real part of the same stiffness.

Some restrictions have to be placed on the parameters in order to obtain a thermodynamically well-behaved model. Bagley and Torvik [15] state that these constraints are

$$k_0 \geqslant 0, \qquad k_\alpha > 0, \qquad l > 0, \qquad \frac{k_\alpha}{l} \geqslant k_0. \tag{6}$$

If the parameter l is set to zero the loss factor will be large at high frequencies, as is the case for the traditional viscous damper. There will be no damping if $k_\alpha/l = k_0$.

Different methods to solve the differential equations which are obtained when the fractional derivative model is used have been proposed. Padovan [16] and Enelund and Olsson [17] presented time stepping algorithms. Bagley and Torvik [12] solved the equations in the Laplace domain. A modal synthesis method was studied by Fenander [18]. Here a time stepping algorithm will be used.

3. RAILPAD MODELS

Three different railpad models have been studied. The parameters of the models have been chosen to describe the studded rubber railpads presently used in Sweden. Laboratory measurements on such railpads have been performed by Thompson and van Vliet [19]. Both laboratory measurements and measurements in a complete track have been reported by Fenander [10].

The easiest way to model the stiffness and the damping of railpads is to use a constant stiffness k_v and a damping force which is proportional to deformation rate, with proportionality constant c_v. This traditional model is here called the viscous model. The relationship between a force $f(t)$ and the corresponding elongation $x(t)$ for the viscous model is written

$$f(t) = k_v x(t) + c_v \mathrm{D}x(t). \tag{7}$$

For harmonic loading a constant complex-valued stiffness may be used in the frequency domain to describe damping. This model, the hysteretic model, is not studied here because it is non-causal in the time domain.

The equations for the spring element in Figure 1, when it is modelled by use of the viscous model, can be written

$$\begin{pmatrix} k_v & -k_v \\ -k_v & k_v \end{pmatrix} \begin{pmatrix} x_1 \\ x_2 \end{pmatrix} + \begin{pmatrix} c_v & -c_v \\ -c_v & c_v \end{pmatrix} \begin{pmatrix} \mathrm{D}x_1 \\ \mathrm{D}x_2 \end{pmatrix} = \begin{pmatrix} f_1 \\ f_2 \end{pmatrix}. \tag{8}$$

Here x_1 and x_2 are the nodal displacements at the ends of the spring element, and f_1 and f_2 are the corresponding nodal forces acting on the element.

As real railpads are non-linear, the values of the parameters in the viscous model will depend on the static preload of the railpads. Here two sets of parameters, corresponding to two levels of preload on one railpad, have been considered. The lower preload level, 20 kN, corresponds to a non-loaded track where only two fastening clips apply load to one railpad. The higher preload level, 80 kN, may be found under a train wheel. The

Figure 1. Spring element with nodal displacements x_1 and x_2 and nodal forces f_1 and f_2.

TABLE 1

Viscous railpad model parameters for two different preloads F_p, fitted to dynamic laboratory measurements

F_p(kN)	k_v(MN/m)	c_v(kNs/m)
20	80	6·0
80	800	30

parameters in the viscous railpad model were determined to fit the measurement data given by Thompson and van Vliet [19], and also by Fenander [10], for these preload levels. Measurement data were given in the frequency range 50–1000 Hz, at frequencies 1 Hz apart. The Rosenbrock optimization method, as described by Fenander [10], was used to determine the parameters, given in Table 1.

To get a railpad model which better takes into account the frequency-dependence of the stiffness and loss factor of the railpads, the fractional derivative model can be used. The relationship between a force $f(t)$ and the corresponding elongation $x(t)$ will then be that of equation (1). For the spring element in Figure 1 the equations become

$$\begin{pmatrix} k_0 & -k_0 \\ -k_0 & k_0 \end{pmatrix}\begin{pmatrix} x_1 \\ x_2 \end{pmatrix} + \begin{pmatrix} k_\alpha & -k_\alpha \\ -k_\alpha & k_\alpha \end{pmatrix}\begin{pmatrix} \mathrm{D}^\alpha x_1 \\ \mathrm{D}^\alpha x_2 \end{pmatrix} = \begin{pmatrix} f_1 \\ f_2 \end{pmatrix} + \begin{pmatrix} l & 0 \\ 0 & l \end{pmatrix}\begin{pmatrix} \mathrm{D}^\alpha f_1 \\ \mathrm{D}^\alpha f_2 \end{pmatrix}. \tag{9}$$

Two different levels of preload have been studied for the fractional derivative model as well. The fractional derivative model parameters determined by Fenander [10] for the preloads 20 and 80 kN have been used. The parameters are listed in Table 2.

As real railpads are non-linear, a non-linear model has been implemented as well. Thompson and van Vliet [19] measured the compression of a railpad as a function of static loading up to 80 kN. The relationship between force and elongation has here been assumed to be the same in tension as in compression. A third-degree polynomial has been fitted to the static load-deflection curve obtained by Thompson and van Vliet and has been assumed to be valid also for dynamic loading. The damping force has been taken to be proportional to deformation rate. The relationship between a force $f(t)$ and the corresponding elongation $x(t)$ in the non-linear model can then be written as

$$f(t) = k_1 x(t) + k_3 x^3(t) + c_n \mathrm{D}x(t). \tag{10}$$

The corresponding equations for the spring element in Figure 1 are

$$\begin{pmatrix} k_1 & -k_1 \\ -k_1 & k_1 \end{pmatrix}\begin{pmatrix} x_1 \\ x_2 \end{pmatrix} + \begin{pmatrix} k_3 & 0 \\ 0 & k_3 \end{pmatrix}\begin{pmatrix} (x_1 - x_2)^3 \\ (x_2 - x_1)^3 \end{pmatrix} + \begin{pmatrix} c_n & -c_n \\ -c_n & c_n \end{pmatrix}\begin{pmatrix} \mathrm{D}x_1 \\ \mathrm{D}x_2 \end{pmatrix} = \begin{pmatrix} f_1 \\ f_2 \end{pmatrix}. \tag{11}$$

TABLE 2

Fractional derivative railpad model parameters for two different preloads F_p, fitted to dynamic laboratory measurements

F_p(kN)	α	k_0(MN/m)	k_α(MNs$^\alpha$/m)	l(s$^\alpha$)
20	0·49	54	0·61	$0{\cdot}69 \times 10^{-9}$
80	0·23	480	57	$6{\cdot}4 \times 10^{-3}$

TABLE 3

Non-linear railpad model parameters fitted to laboratory measurements

k_1(MN/m)	k_3(TN/m^3)	c_n(kNs/m)
12	3·5	6·0

The parameters obtained for the non-linear model are given in Table 3. Since the damping cannot be determined from static measurements, the damping constant c_n has been chosen to be equal to the damping constant in the viscous model for the preload 20 kN.

4. TRACK MODEL

Assuming that the track and the load from the train are symmetric, only half of the track need be included in a model. In the examples a rather simple track model has been used, since the aim was to study the influence of the railpad models on the response of the track. The length of the track model is eight sleeper bays, as shown in Figure 2. The rail is modelled by use of standard Euler–Bernoulli beam elements with consistent mass matrices, see, e.g., reference [20]. In each sleeper bay the rail is divided into four equal beam elements, with bending stiffness $EI = 6{\cdot}11$ MNm^2 and mass per unit length $m_r = 60{\cdot}34$ kg/m. These data correspond to the rail type UIC60. The sleepers are situated at a distance $L = 0{\cdot}70$ m apart and are modelled as discrete masses $m_s = 125$ kg, which is half the mass of the concrete sleeper used in Sweden. Each sleeper mass is connected to the rail via one of the three railpad models described. The ballast under each sleeper is modelled as a damped spring by use of the viscous model in equation (7) with stiffness $k_b = 20$ MN/m and damping constant $c_b = 20$ kNs/m. The load on the track model is a force P traversing the track at a constant speed v.

The equations of motion for the different elements of the model are assembled into a system of structural equations for the whole track. The internal nodal forces are then eliminated. In the case of the viscous railpad model the system of equations is

$$\mathbf{M}D^2\mathbf{d} + \mathbf{C}D\mathbf{d} + \mathbf{K}\mathbf{d} = \mathbf{F}, \tag{12}$$

where $\mathbf{M}$ is the mass matrix, $\mathbf{C}$ is the damping matrix, $\mathbf{K}$ is the stiffness matrix, and $\mathbf{d}$ is the vector of nodal displacements. The vector $\mathbf{F}$ contains the applied load. The mass matrix has contributions from the beam element mass matrices and it also contains the sleeper masses. The stiffness matrix has contributions from all parts of the track, while the damping matrix only has contributions from the ballast springs and from the viscous railpad model.

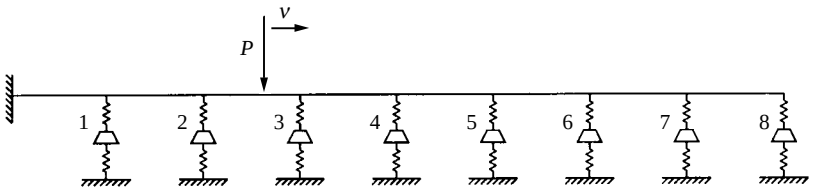

Figure 2. Track model traversed by force P at constant speed v.

In the cases with the fractional derivative railpad model and the non-linear railpad model, equation (12) has to be modified. For the fractional derivative railpad model, the internal nodal forces have been eliminated, but the fractional derivatives of the forces through the railpads have been accounted for as internal loads on the right-hand side of the structural equation. In this manner the order of the equations is not raised, as would have been the case, if the fractional derivatives of the internal nodal forces had been eliminated by applying a fractional order derivative to Newton's second law, see, e.g. reference [21]. The fractional derivatives of the displacements of the railpads turn up on the left-hand side,

$$\mathbf{M}\mathrm{D}^2\mathbf{d} + \mathbf{C}\mathrm{D}\mathbf{d} + \mathbf{K}_\alpha \mathrm{D}^\alpha\mathbf{d} + \mathbf{K}\mathbf{d} = \mathbf{F} + \mathbf{L}\,\mathrm{D}^\alpha\mathbf{f}. \tag{13}$$

Here the matrix $\mathbf{K}_\alpha$ contains the element matrices with the fractional derivative railpad model parameters k_α from equation (9). In the matrix $\mathbf{L}$ the parameters l from equation (9) appear on the diagonal at places corresponding to the nodes of the railpad elements. Further, $\mathrm{D}^\alpha\mathbf{f}$ are the fractional derivatives of the force through the railpads. The damping matrix $\mathbf{C}$ now has contributions only from the ballast damping, which appear in the diagonal. In the stiffness matrix $\mathbf{K}$ the stiffness k_v of the viscous railpad model has been replaced by the stiffness factor k_0 of the fractional derivative railpad model.

The initial conditions needed in equation (13) may be found by applying the Laplace transform to the equation [13, 21]. It is then found that initial conditions are needed for the displacement, $\mathbf{d}(0)$, and the velocity, $\mathrm{D}\mathbf{d}(0)$. Initial conditions for $\mathrm{D}^{\alpha-1}\mathbf{d}(0)$ and $\mathrm{D}^{\alpha-1}\mathbf{f}(0)$ are also needed. The latter two are fractional integrals with lower and upper limits equal to zero, and they vanish for any reasonable displacement or force.

For the non-linear model, the non-linear term has been included on the left-hand side of equation (12),

$$\mathbf{M}\mathrm{D}^2\mathbf{d} + \mathbf{C}\mathrm{D}\mathbf{d} + \mathbf{K}\mathbf{d} + \mathbf{K}_3(\Delta\mathbf{d})^3 = \mathbf{F}. \tag{14}$$

Here the matrix $\mathbf{K}_3$ consists of the spring element matrices containing the parameters k_3 in equation (11). The vector $(\Delta\mathbf{d})^3$ contains the corresponding railpad shortenings and elongations, i.e., the differences between the nodal displacements at the ends of each railpad, raised to the power three. As in the viscous case, the damping matrix C will contain contributions from the railpads and the ballast.

5. ALGORITHM

To calculate the response of the track to the moving load, several different numerical methods may be used. Here a Newmark method has been exploited [20]. The nodal displacement $\mathbf{d}_{i+1}$ in step $i+1$ is then obtained as

$$\mathbf{d}_{i+1} = \mathbf{d}_i + \Delta t(\mathrm{D}\mathbf{d})_i + \frac{(\Delta t)^2}{2}(\mathrm{D}^2\mathbf{d})_i, \tag{15}$$

where the index i denotes time step i and Δt is the length of the time step. The nodal velocity $(\mathrm{D}\mathbf{d})_{i+1}$ in step $i+1$ is written as

$$(\mathrm{D}\mathbf{d})_{i+1} = (\mathrm{D}\mathbf{d})_i + \frac{\Delta t}{2}((\mathrm{D}^2\mathbf{d})_i + (\mathrm{D}^2\mathbf{d})_{i+1}). \tag{16}$$

To get expressions for the fractional derivatives in step $i+1$ an alternative definition of the fractional derivative is used [13],

$$\mathrm{D}^\alpha x(t) = \lim_{N\to\infty} \frac{(t/N)^{-\alpha}}{\Gamma(-\alpha)} \sum_{j=0}^{N-1} \frac{\Gamma(j-\alpha)}{\Gamma(j+1)} x\left(t - j\frac{t}{N}\right). \tag{17}$$

By omitting the limit procedure in the definition, an expression which is suitable for numerical calculations of the fractional derivatives is obtained [13, 21]. The time step $\Delta t = t/N$ is introduced and the ratio of gamma functions is denoted by $\mathrm{B}_\alpha(j)$,

$$\mathrm{B}_\alpha(j) = \frac{\Gamma(j-\alpha)}{\Gamma(-\alpha)\Gamma(j+1)}. \tag{18}$$

An expression for the fractional derivative of the displacement, $(\mathrm{D}^\alpha \mathbf{d})_{i+1}$, in step $i+1$ is then obtained as

$$(\mathrm{D}^\alpha \mathbf{d})_{i+1} = \frac{1}{(\Delta t)^\alpha}\left(\mathbf{d}_{i+1} + \sum_{j=1}^{i} \mathrm{B}_\alpha(j)\mathbf{d}_{i+1-j}\right). \tag{19}$$

The values of the function $\mathrm{B}_\alpha(j)$ may be calculated recursively, due to the properties of the gamma function,

$$\mathrm{B}_\alpha(j) = \frac{(j-1-\alpha)}{j}\,\mathrm{B}_\alpha(j-1). \tag{20}$$

For large times, i.e., when the step number i is large, the sums in equation (19) will contain a large number of terms. However, the function $\mathrm{B}_\alpha(j)$ is small for large j and the sums may be truncated. Here a maximum of 10,000 terms have been included in each sum. Including more terms in the sums was found not to alter the response of the track.

When everything is known in step i, the new displacement $\mathbf{d}_{i+1}$ in step $i+1$ may be calculated from equation (15). Thereafter, the new fractional derivative of the displacement, $(\mathrm{D}^\alpha \mathbf{d})_{i+1}$, may be obtained from equation (19). A similar expression can be written for the fractional derivative of the force through the railpad, $(\mathrm{D}_\alpha \mathbf{f})_{i+1}$,

$$(\mathrm{D}^\alpha \mathbf{f})_{i+1} = \frac{1}{(\Delta t)^\alpha}\left(\mathbf{f}_{i+1} + \sum_{j=1}^{i} \mathrm{B}_\alpha(j)\mathbf{f}_{i+1-j}\right). \tag{21}$$

As compared to equation (19) a problem here is that the force $\mathbf{f}_{i+1}$ through the railpad at step $i+1$ is not yet known. It may be obtained with the aid of equation (9). Considering, e.g., the force f_1 in the spring element in Figure 1, equation (9) gives

$$f_{1,i+1} + l(\mathrm{D}^\alpha f_1)_{i+1} = k_0 x_{1,i+1} - k_0 x_{2,i+1} + k_\alpha(\mathrm{D}^\alpha x_1)_{i+1} - k_\alpha(\mathrm{D}^\alpha x_2)_{i+1}. \tag{22}$$

The displacement $\mathbf{d}_{i+1}$, where the spring element nodal displacement $x_{1,i+1}$ and $x_{2,i+1}$ are included, is already calculated, as is the fractional derivative of the displacement $(\mathrm{D}^\alpha \mathbf{d})_{i+1}$. The fractional derivative of the force, $(\mathrm{D}^\alpha \mathbf{f})_{i+1}$, is taken from equation (21), and inserted into equation (22). The updated value of the force $\mathbf{f}_{i+1}$ may then be solved for in equation (22). The fractional derivative of the force, $(\mathrm{D}^\alpha \mathbf{f})_{i+1}$, is thereafter obtained from equation (21).

An algorithm for the track calculations may now be set up as follows. First, the new displacement is calculated from equation (15). In the case of the fractional derivative railpad model, the new fractional derivative of the displacement is calculated from equation (19). Thereafter the force through the railpad and its fractional derivative are calculated from equations (22) and (21). For all railpad models, the applied load $\mathbf{F}$ is calculated from the present value and the present location of the moving load and the shape functions of the beam elements [20]. The velocity is taken from equation (16) and

inserted, together with the displacements, the fractional derivatives (if present) and the applied load, into the structural equation (12), (13) or (14), respectively, depending on the railpad model. Then the updated acceleration is obtained from this equation. Eventually the velocity is updated by equation (16).

Since the track is assumed to be at rest before the moving load enters, the initial conditions are taken as homogeneous.

6. TRACK RESPONSE

The response of the track model in Figure 2 to a load traversing the track has been calculated. In all calculations a time step $\Delta t = 10^{-7}$s has been used. Using a smaller time step gave the same results as those reported. For the viscous railpad model a larger time step could be used, but for the other railpad models a larger time step resulted in a small change in the calculated response.

First the fractional derivative railpad model was investigated. The load was chosen to be $P = 20$ kN and it traversed the track at a speed $v = 70$ km/h. In Figure 3 the vertical deflection δ of the rail under the moving load divided by the load P, is shown when the two different sets of parameters in Table 2 are used. As expected the deflection is smaller when the set of parameters corresponding to the higher preload is used, since the railpad is stiffer for a higher preload. This can also be seen in Figure 4 where the compression Δ of the fifth railpad in the track model, divided by the load P, is shown. If another value of the load P had been used the results in Figures 3 and 4 would have been the same since the model is linear. Also other velocities have been tried. Increasing the speed to, e.g., $v = 160$ km/h gives only a small increase of the deflection of the rail, as is shown in Figure 5.

The viscous model with the two sets of parameters in Table 1 has also been used. In Figure 6 the vertical deflection δ of the rail under the moving load, divided by the load P, is shown. Comparing the deflections when the fractional derivative railpad model and the viscous railpad model are used, it is seen that for the parameters corresponding to the higher preload the deflections are very close. For the parameters corresponding to the

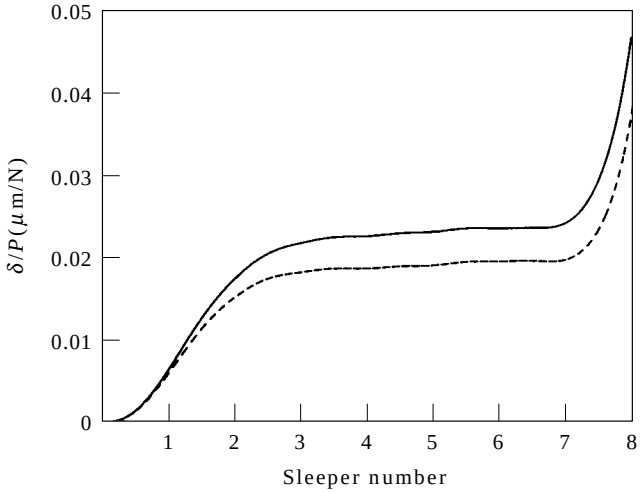

Figure 3. Calculated vertical deflection δ of rail divided by load P as function of load position along track in Figure 2. Fractional derivative railpad model is used. ═══, Railpad parameters determined for preload 20 kN; – – –, railpad parameters determined for preload 80 kN. Load speed $v = 70$ km/h. Time to traverse track model is 0·288 s.

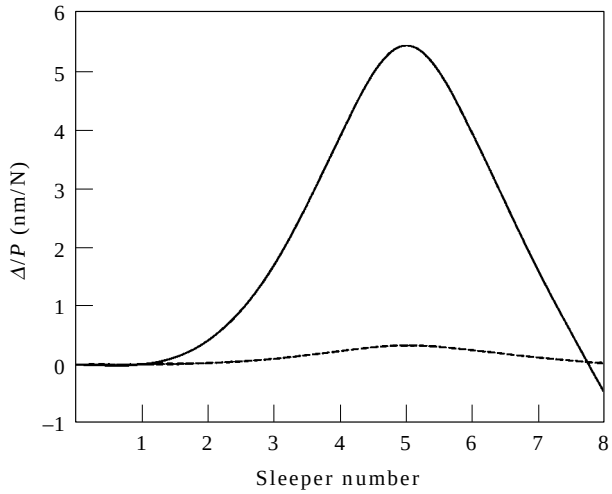

Figure 4. Calculated compression Δ of fifth railpad divided by load P as function of load position along track in Figure 2. Fractional derivative railpad model is used. ——, Railpad parameters determined for preload 20 kN; – – – railpad parameters determined for preload 80 kN. Load speed $v = 70$ km/h. Time to traverse track model is 0·288 s.

lower preload, the fractional derivative railpad model gives a larger deflection than the viscous model.

The compression of the fifth railpad when the viscous model is used is shown in Figure 7. For the parameter sets corresponding to the lower preload the compression of the viscous railpad model is smaller than the compression of the fractional derivative railpad model. For the parameter sets corresponding to the higher preload, on the other hand, the compression of the viscous railpad model is larger than the compression of the fractional derivative railpad model. Also in the case of the viscous model the influence of increasing the load speed to $v = 160$ km/h is very small.

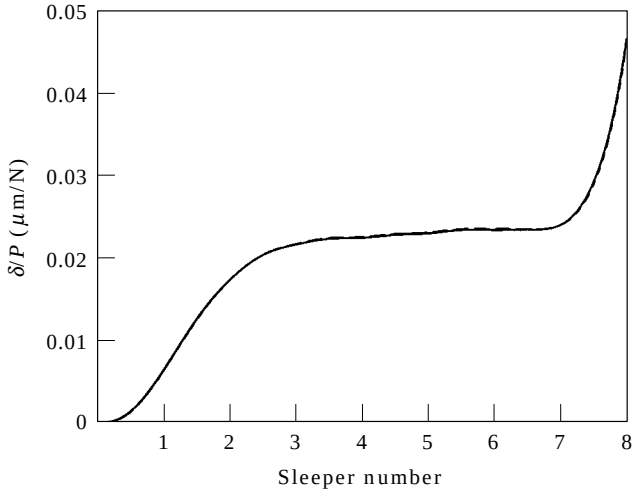

Figure 5. Calculated vertical deflection δ of rail divided by load P as function of load position along track in Figure 2. Fractional derivative railpad model, railpad parameters determined for preload 20 kN. ═══, Load speed $v = 70$ km/h, time to traverse track model is 0·288 s; – – –, (almost coinciding) load speed $v = 160$ km/h, traversing time is 0·126 s.

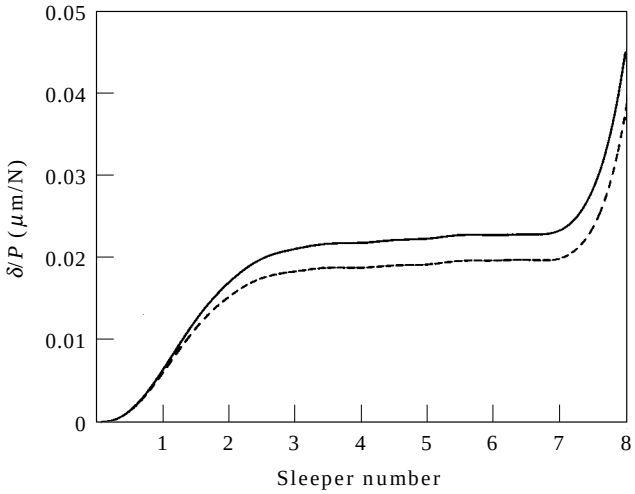

Figure 6. Calculated vertical deflection δ of rail divided by load P as function of load position along track in Figure 2. Viscous railpad model is used. ——, Railpad parameters determined for preload 20 kN; – – –, railpad parameters determined for preload 80 kN. Load speed is $v = 70$ km/h, Time to traverse track model is 0·288 s.

Since the different sets of parameters of the linear railpad models give such different results, a non-linear railpad model has also been implemented. The non-linear railpad model with the set of parameters given in Table 3 has been used. The resulting deflection of the rail, divided by the load P, is shown in Figure 8 when the load is $P = 20$ kN and $P = 80$ kN, respectively. As seen, the higher load gives a smaller relative deflection than the lower load, since the stiffness of the non-linear railpad model is higher at higher loads. The non-linear railpad model gives a larger deflection than the linear railpad models. One reason for this is that the parameters are not determined form the same measurement data. The data for the linear railpad models have been obtained from dynamic measurements with a static preload. The non-linear model, on the other hand, has a varying stiffness

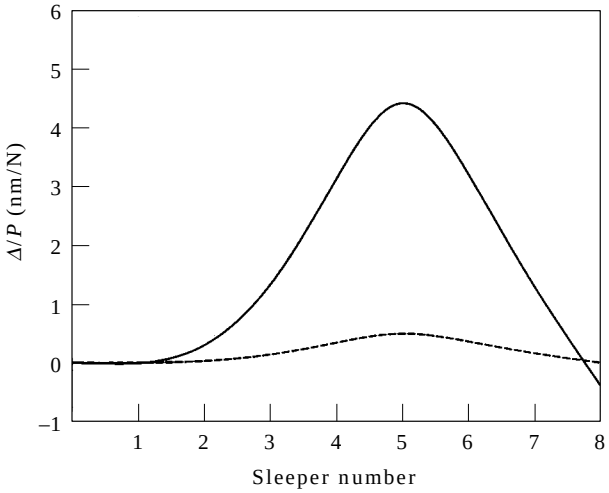

Figure 7. Calculated compression Δ of fifth railpad divided by load P as function of load position along track in Figure 2. Viscous railpad model is used. ═══, Railpad parameters determined for preload 20 kN; – – –, railpad parameters determined for preload 80 kN. Load speed $v = 70$ km/h. Time to traverse track model is 0·288 s.

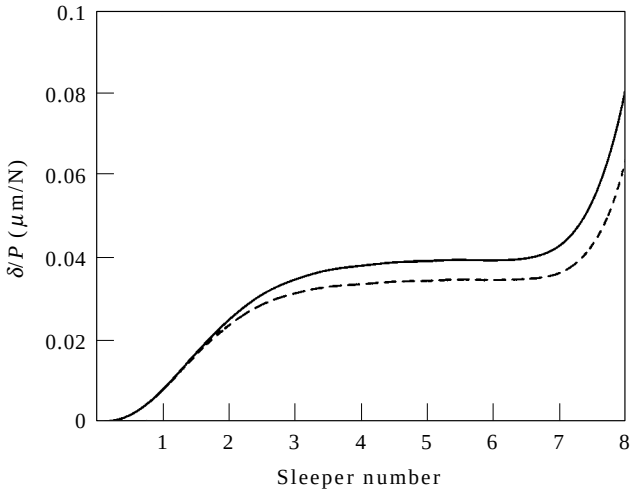

Figure 8. Calculated vertical deflection δ of rail divided by load P as function of load position along track in Figure 2. Non-linear railpad model is used. ——, $P = 20$ kN; – – –, $P = 80$ kN. Load speed $v = 70$ km/h. Time to traverse track model is 0·288 s.

obtained from static measurements. The ratio between the stiffnesses in the static measurement and in the dynamic measurements is about 2·9 at 50 Hz and 4·3 at 500 Hz, independent of preload [19]. When the non-linear railpad model is used, it takes a longer time until the deflection of the rail reaches its plateau value, as compared to when one of the linear railpad models is used.

The compression of the fifth railpad divided by the load, when the non-linear railpad model is used, is shown in Figure 9. As expected, the higher load gives a smaller relative compression than the lower load. As for the linear railpad models, the influence of increasing the speed is very small.

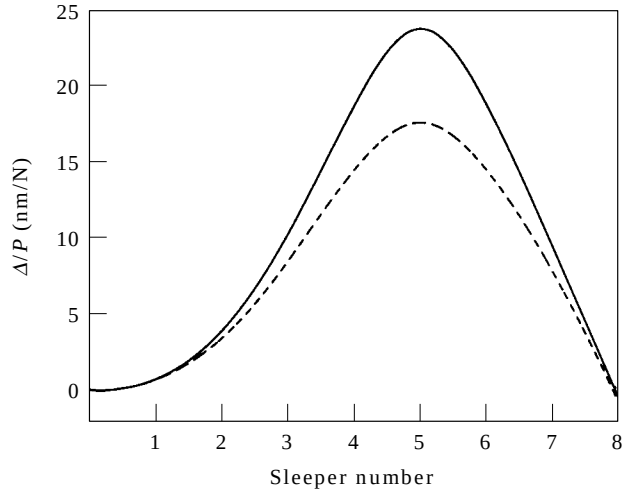

Figure 9. Calculated compression Δ of fifth railpad divided by load P as function of load position along track in Figure 2. Non-linear railpad model is used. ——, Load $P = 20$ kN; – – –, $P = 80$ kN. Load speed $v = 70$ km/h. Time to traverse track model is 0·2888 s.

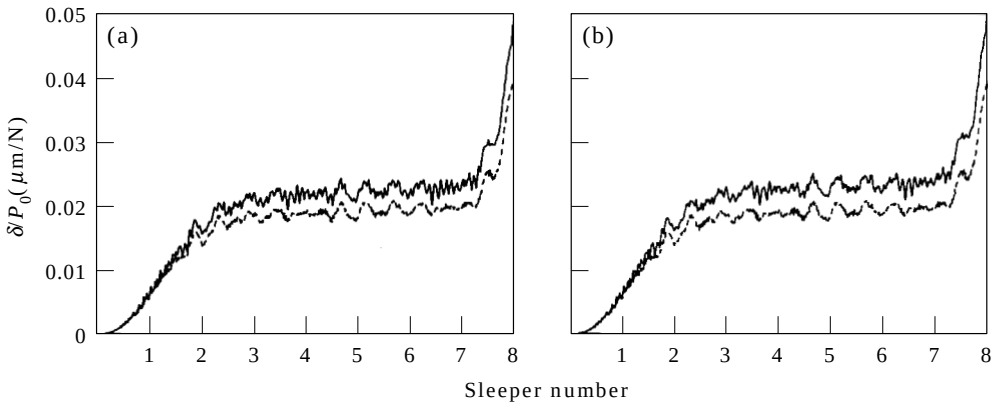

Figure 10. Calculated vertical deflection δ of rail divided by load mean value P_0 as function of load position along track in Figure 2. (a) Viscous railpad model is used; (b) Fractional derivative railpad model is used. ═══. Railpad parameters determined for preload 20 kN; – – – railpad parameters determined for preload 80 kN. Load speed $v = 70$ km/h. Time to traverse track model is 0·288 s.

To study the high frequency behaviour of the linear railpad models the train load has also been modelled as a sample of a stochastic process. A suitable stochastic process can be simulated by use of a cosine series [22],

$$P(t) = P_0 + P_a \sum_{i=1}^{N} \cos(\omega_i t + \varphi_i). \tag{23}$$

The mean value of the process is P_0. Further, N is the number of cosine terms and $\omega_i = 2\pi f_i$ are the equally spaced angular frequencies. In the examples the equidistance of the frequencies f_i is 10 Hz in the range 50–1000 Hz, which is the range of the fit of the railpad parameters. The mutually independent phase angles φ_i are randomly and uniformly distributed between 0 and 2π. The amplitude P_a is chosen to make the standard deviation P_{std} of the process equal to 10 per cent of the mean value, i.e., $P_{std} = P_a\sqrt{N/2} = 0{\cdot}10\ P_0$.

The same sample of the process has been used as a load for the fractional derivative railpad model and for the viscous railpad model. In Figure 10 the resulting deflection δ

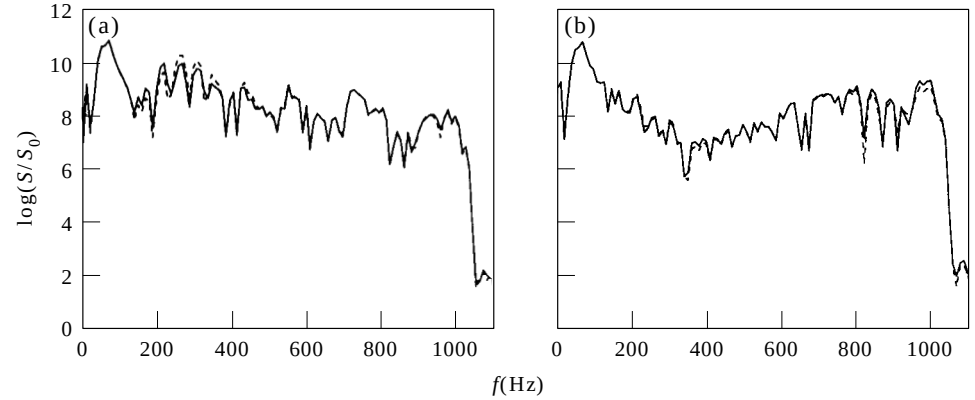

Figure 11. Calculated one-sided spectral density of vertical deflection δ between sleepers 3 and 7 shown in Figure 10. (a) Railpad parameters determined for preload 20 kN; (b) railpad parameters determined for preload 80 kN. ═══, Fractional derivative railpad model; – – –, viscous railpad model. Reference value is $S_0 = 10^{-22}$ m²s/N².

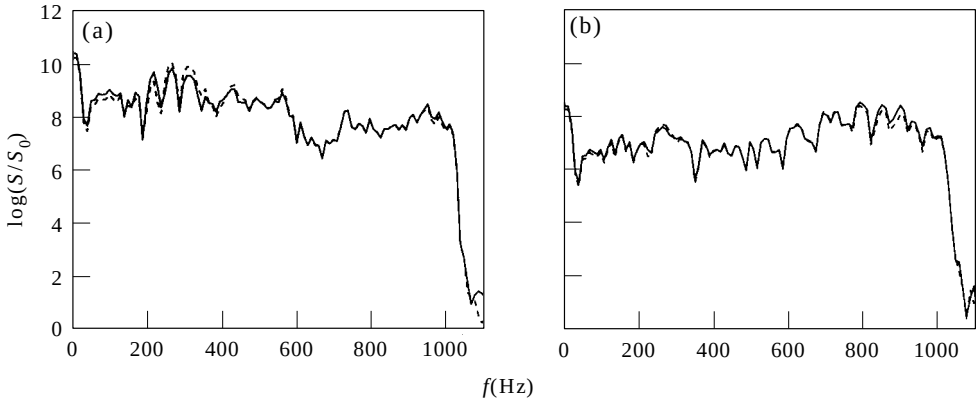

Figure 12. Calculated one-sided spectral density of compression Δ of fifth railpad. (a) Railpad parameters determined for preload 20 kN; (b) railpad parameters determined for preload 80 kN. ═══, Fractional derivative railpad model; – – –, viscous railpad model. Reference value is $S_0 = 10^{-22}$ m^{2}s/N^2.

of the rail under the moving load, divided by the mean value of the load P_0, is shown for the different sets of parameters. The differences between the viscous railpad model and the fractional derivative railpad model are the same as for the case with a constant load.

The spectral density of the deflection of the rail between sleeper numbers 3 and 7 has been calculated and is shown in Figure 11. The spectral density of the whole compression of the fifth railpad is shown in Figure 12. The results for the fractional derivative railpad model are very close to the results for the viscous railpad model. The main difference between the spectral density of the vertical deflection δ and that of the compression Δ is that the spectral density of the vertical deflection δ has a peak at 70 Hz. This frequency corresponds to an eigenmode of the track model where the rail and the sleeper masses move in phase on the ballast, i.e., the railpads are deformed relatively little. This eigenfrequency is the same for all the linear railpad models.

7. CONCLUDING REMARKS

A fractional derivative railpad model has been included in a railway track model. The method to include a fractional derivative model in the track model may also be used for other structures. The response of the track model to a load traversing the track at a constant speed has been calculated.

For comparison a viscous railpad model has also been used. The parameters of these two railpad models have been determined to fit the same measurement data. Two sets of parameters for each railpad model have been used, corresponding to the preloads 20 and 80 kN, respectively. For the parameter sets corresponding to the lower preload, the viscous railpad model was seen to give a smaller deflection of the rail and a smaller railpad compression than the fractional derivative railpad model. For the parameter sets corresponding to the higher preload, on the other hand, the viscous railpad model gave a somewhat larger railpad compression than the fractional derivative railpad model, while the deflections of the rail were similar. In the case of a random force the spectral densities of the rail deflection and of the railpad compression were similar for the fractional derivative railpad model and the viscous railpad model.

The differences between the results when using the viscous railpad model and the fractional derivative railpad model were small. For other applications, however, the difference between a fractional derivative model and a viscous model may be important.

It should be noted that the calculation time is large when the fractional derivative railpad model is used. In order to make calculations with the fractional derivative model more efficient, some improvements in the time integration method have to be made, e.g., by introducing a variable length of the time step.

As real railpads are non-linear, a non-linear railpad model was studied as well. The non-linear railpad model gave a larger deflection than the linear railpad models. One reason for this is that the parameters of the non-linear railpad model were determined by use of data from static measurements, while the parameters of the linear railpad models were determined by use of frequency-dependent data. The non-linear model gave a slightly different form of the deflection curve than that obtained by the linear railpad models. Increasing the load when the non-linear railpad model was used did not give a correspondingly larger increase of the deflection, as expected. The non-linearity will be more important when a better vehicle model is included and when the possibility of loss of contact between the wheel and the rail is considered [5], because then the load on the track will vary considerably. However, the establishment of a reliable non-linear railpad model would require more measurements on actual railpads.

ACKNOWLEDGMENTS

This research has been performed within the Swedish National Centre of Excellence CHARMEC (CHAlmers Railway MEChanics). This centre has been established by the Swedish National Board for Industrial and Technological Development (NUTEK). The concrete sleeper manufacturer Abetong Teknik AB supported the research. Valuable discussions with Dr Jan Henrik Sällström are acknowledged. Dr Tore Dahlberg supervised the work.

REFERENCES

1. K. Knothe and S. L. Grassie 1993 *Vehicle System Dynamics* **22**, 209–262. Modelling of railway track and vehicle/track interaction at high frequencies.
2. S. L. Grassie 1996 *Vehicle System Dynamics Supplement* **25**, 243–262. Models of railway track and vehicle/track interaction at high frequencies: results of benchmark test.
3. R. A. Clark, P. A. Dean, J. A. Elkins and S. G. Newton 1982 *Proceedings of the Institution of Mechanical Engineers*, *Part C*: *Journal of Mechanical Engineering Science* **24**, 65–76. An investigation into the dynamic effects of railway vehicles running on corrugated rails.
4. Z. Cai and G. P. Raymond 1994 *Structural Engineering and Mechanics* **2**, 95–112. Modelling the dynamic response of railway track to wheel/rail impact loading.
5. J. C. O. Nielsen and T. J. S. Abrahamsson 1992 *International Journal for Numerical Methods in Engineering* **33**, 1843–1859. Coupling of physical and modal components for analysis of moving non-linear dynamic systems on general beam structures.
6. S. L. Grassie, R. W. Gregory, D. Harrison and K. L. Johnson 1982 *Journal of Mechanical Engineering Science* **24**, 77–90. The dynamic response of railway track to high frequency vertical excitation.
7. S. L. Grassie and S. J. Cox 1984 *Proceedings of the Institution of Mechanical Engineers*, *Part D*: *Transport Engineering* **198**, 117–124. The dynamic response of railway track with flexible sleepers to high frequency vertical excitation.
8. M. Dalenbring 1995 *Report KTH/FKT/FR*-95/06-*SE*, *Department of Technical Acoustics*, *Royal Institute of Technology*, *Stockholm*, *Sweden*. A study of the effect of track parameter changes on vertical rail vibrations.
9. M. Fermér and J. C. O. Nielsen 1995 *Proceedings of the Institution of Mechanical Engineers*, *Part F*: *Journal of Rail and Rapid Transit* **209**, 39–47. Vertical interaction between train and track with soft and stiff railpads—full-scale experiments and theory.
10. Å. Fenander 1997 *Proceedings of the Institution of Mechanical Engineers*, *Part F*: *Journal of Rail and Rapid Transit* **211**, 51–62. Frequency dependent stiffness and damping of railpads.

11. S. H. Crandall 1970 *Journal of Sound and Vibration* **11**, 3–18. The role of damping in vibration theory.
12. R. L. Bagley and P. J. Torvik 1983 *AIAA Journal* **21**, 741–748. Fractional calculus—a different approach to the analysis of viscoelastically damped structures.
13. K. B. Oldham and J. Spanier 1974 *The Fractional Calculus*. New York and London: Academic Press.
14. R. L. Bagley and R. A. Calico 1991 *Journal of Guidance, Control & Dynamics* **14**, 304–311. Fractional order state equations for the control of viscoelastically damped structures.
15. R. L. Bagley and P. J. Torvik 1986 *Journal of Rheology* **30**, 133–155. On the fractional calculus model of viscoelastic behaviour.
16. J. Padovan 1987 *Computational Mechanics* **2**, 271–287. Computational algorithms for FE formulations involving fractional operators.
17. M. Enelund and P. Olsson 1995 In *Proceedings 36th AIAA/ASME/ASCE/AHS/ASC Structures, Structural Dynamics and Materials Conference, part* 1, 207–220. *Washington, DC: AIAA*. Damping described by fading memory models.
18. Å. Fenander 1996 *AIAA Journal* **34**, 1051–1058. Model synthesis when modelling damping by use of fractonal derivatives.
19. D. J. Thompson and W. J. van Vliet 1996 *TNO-report TPD-HAG-RPT-960066, TNO Institute of Applied Physics, Delft, The Netherlands*. Measurements of the high frequency dynamic properties of Swedish rail pads.
20. R. D. Cook, D. S. Malkus and M. E. Plesha 1989 *Concepts and Applications of Finite Element Analysis*. New York: Wiley; third edition.
21. M. Enelund, Å. Fenander and P. Olsson 1997 *AIAA Journal* **35**, 1356–1362. A fractional integral formulation of constitutive equations of viscoelasticity.
22. M. Shinozuka 1972 *Computers & Structures* **2**, 855–874. Monte Carlo solution of structural dynamics.